



# Mutagenesis enhances gellan gum production by a novel *Sphingomonas* spp.: upstream optimization, kinetic modeling, and structural and physico-functional evaluation

Manoj J. Dev<sup>1,2</sup> · Girish B. Mahajan<sup>2</sup> · Rahul G. Warke<sup>2</sup> · Gangadhar M. Warke<sup>2</sup> · Tanuja A. Patil<sup>2</sup> · Milan R. Satardekar<sup>2</sup> · Rachana C. Dalvi<sup>2</sup> · Rekha S. Singhal<sup>1</sup>

Received: 24 February 2023 / Revised: 11 June 2023 / Accepted: 7 July 2023 / Published online: 26 July 2023

© The Author(s), under exclusive licence to Springer Nature Switzerland AG 2023

## Abstract

Gellan gum (GG) has gained tremendous attention owing to its diversified applications. However, its high production and hence market cost are still a bottleneck in its widespread utilization. In the present study, high GG producing mutant of *Sphingomonas* spp. was developed by random mutagenesis using ethyl methylsulphonate (EMS) for industrial fermentation and identified as *Sphingomonas trueperi* after 16S rRNA and matrix-assisted laser desorption/ionization-time of flight mass spectrometry (MALDI-TOF-MS) analysis. The fermentation conditions such as pH, temperature, and inoculum ratio were optimized by one factor at a time (OFAT) followed by screening of medium components by the Plackett–Burman statistical design. The most critical nutrients were further optimized by response surface methodology for maximizing GG production. The effect of dissolved oxygen tension in bioreactor on cell growth, substrate consumption, GG production, and batch productivity was elucidated. The highest GG titer ( $23 \pm 2.4$  g/L) was attained in optimized medium at 10% inoculum ( $6.45 \pm 0.5$  log cfu/mL) under controlled fermentation conditions of pH (7), temperature (30 °C), agitation (300–600 rpm), and aeration (0.5–2.0 SLPM) at  $22 \pm 2\%$  dissolved oxygen tension in a 10-L bioreactor. Kinetic modeling of optimized batch process revealed that logistic growth model could best explain biomass accumulation, while GG formation and substrate consumption were best explained by Luedeking–Piret and exponential decay model, respectively. Structural and physico-functional features of GG produced by mutant *Sphingomonas* spp. were characterized by HPLC, FTIR, NMR, DSC, TGA, GPC, SEM, and rheological analysis. The higher productivity (0.51 g/L/h) under optimized fermentation conditions suggests potential consideration of mutant and process for commercial utilization.

**Keywords** *Sphingomonas* · Gellan gum · Mutagenesis · Fermentation · Physico-functional properties

## Introduction

Gellan gum (GG) is a linear anionic exopolysaccharide (EPS) having glucose: rhamnose: glucuronic acid in 2:1:1 ratio along with acetyl and glycerate substitution in a repeating tetra-saccharide unit (O'Neill et al. 1983). It is produced by fermentation using non-pathogenic bacteria *Sphingomonas paucimobilis* under controlled fermentation

conditions. In its native form, GG is categorized as “high acyl” which forms soft and elastic gels. Deacylation by alkali treatment yields “low acyl” GG which forms hard and brittle gels (O'Neill et al. 1983; Kuo et al. 1986; Morris et al. 2012). The stability over wide range of pH and temperature along with tunable rheological properties makes GG a material of choice as thickener, stabilizer, taste controller, texture modifier, gelling agent, and emulsifier in a wide spectrum of industries such as in food, pharmaceutical, biomedical, personnel care, and oil recovery industries (Fialho et al. 2008; Dev et al. 2022).

The global industrial demand of GG is rising continuously with approximately 12% compound annual growth rate (CAGR). Higher demand, lower industrial productivity (g/L/h), and high production cost are the reasons for higher price of GG (up to 150 \$/kg) which restricts its preferential

✉ Rekha S. Singhal  
rsinghal7@rediffmail.com

<sup>1</sup> Food Engineering and Technology Department, Institute of Chemical Technology, Mumbai 400019, India

<sup>2</sup> Department of Microbiology, HiMedia Laboratories Pvt. Ltd, Mumbai, India

use over other competitive hydrocolloids such as agar and xanthan (Wu et al. 2011; Li et al. 2019; Viswanathan et al. 2020). To overcome the current scenario, different approaches such as strain development (Lobas et al. 1992; Monteiro et al. 1992; Fialho et al. 2008), media optimization (Nampoothiri et al. 2003; Bajaj et al. 2007; Banik et al. 2007; Huang et al. 2012), fermentation, and downstream process optimization (West and Fullenkamp 2001; Kanari et al. 2002; Banik and Santhiagu 2006; Giavasis et al. 2006; Zhu et al. 2011; Huang et al. 2012; Viswanathan et al. 2020) have been attempted and are still ongoing. Previous attempts have enlightened the researchers for better understanding of challenges in the fermentative and downstream operations of GG bioprocess.

Random and targeted mutations for strain development have been long explored for improving the yield of GG. Although, such attempts have added significant new information on genetic assembly of *Sphingomonas* spp., but it has not persuasively translated in improving the yield of GG from an industrial perspective (Lobas et al. 1992; Dev et al. 2022). Random mutagenesis has been preferred in industrial fermentation owing to its simple, time saving, cost-effectiveness, and capacity to generate stable mutants (Lobas et al. 1992; Wu et al. 2011; Zhu et al. 2011). Approaches such as UV or gamma radiation treatment or chemical mutagenesis using chemicals such as ethyl methylsulphonate (EMS) are promising ways for developing *Sphingomonas* mutant with desired capabilities of industrial fermentation. Such physical or chemical treatment generates mutants by creating lesions, or irreversibly altering base sequences of microbial genome (Foster 1991). Such mutational breeding have been reported to improve the EPS production in *Cordyceps militaris* SU5-08 and *Xanthomonas campestris* (Lin et al. 2012; Kothari et al. 2014). Lobas et al. (1992) have developed an industrial mutant *Sphingomonas paucimobilis* E2 (DSM 6314) by EMS treatment from wild type strain *Auromonas elodea* (ATCC 31461) and showed an impressive increase in productivity from 0.04 to 0.17 g/L/h. Similarly, Li et al. (2019) used a combined approach of UV radiation and EMS treatment for elevating the production of GG in *Sphingomonas elodea* by 14.4% (1.35 g/L) over the wild type strain. Although, there has been little improvement in gellan gum production by random mutational breeding, and the approach has been successfully worked for other similar microbial polysaccharide such as pullulan. Recently, Li et al. (2023) reported atmospheric and room temperature plasma (ARTP) mediated random mutagenesis and adaptive evolution of *Aureobasidium pullulan* for high production yield of pullulan (162.3 g/L). This confirms efficacy of random mutagenesis in strain development for industrial fermentation.

Although random mutagenesis has been a proven and preferred way to develop stable mutants, it also has certain

disadvantages. Different mutants of bacterial strain from same genus developed by random mutation, under identical culture conditions, can produce EPS like GG with variable structural and hence physico-functional characteristics (Matsuyama et al. 2003; Dertli et al. 2013). Hence, a detailed assessment of structural and functional attributes of the metabolite is crucial in random mutagenesis. Similarly, stable and high productive mutant has to be optimized for media components such as the type and concentration of carbon and nitrogen source, C/N ratio, precursors, and dissolved oxygen tension (DOT) in the bioreactor to accomplish maximum process yield and productivity (Huang et al. 2012; Dev et al. 2022).

Literature reports indicate the efficacy of EMS for random mutational breeding of *Sphingomonas* spp. for improved polysaccharide production as reported earlier (Lobas et al. 1992; Jay et al. 1998; Wu et al. 2011; Li et al. 2019). Hence, EMS treatment was explored in the present study to generate a stable mutant of wild strain *Pseudomonas elodea* NCIMB 12171. The potential mutants were screened based on survival capacity, colony size, extent of mucoidness and pigmentation, generation stability, and GG yield and characterized by 16S rRNA along with MALDI-TOF mass spectroscopic analysis. The EPS produced by mutant strains of *Sphingomonas* spp. was characterized for its composition by HPLC followed by structural analysis by FTIR, NMR, DSC, TGA, molecular weight, and rheological properties and compared with commercial GG. The most promising mutant was taken ahead for GG process development wherein media components were screened and optimized by the Plackett–Burman statistical design for screening variables followed by RCCD for further optimization. The effect of variable dissolved oxygen tension (DOT) on substrate consumption, cell growth, yield of GG, and productivity in the bioreactor has been elucidated. The optimized batch data was used to generate various kinetic parameters such as instantaneous growth rate ( $r_x$ ), instantaneous rate of product formation ( $r_p$ ), instantaneous rate of substrate consumption ( $r_s$ ), and productivity ( $P_r$ ). Different kinetic models were evaluated to understand the kinetics of cell growth, product formation, and substrate utilization by mutant *Sphingomonas* spp.

## Material and methods

### Chemicals and reagents

All the reagents and chemicals were of analytical grade and kindly provided by HiMedia Laboratories Private Limited (Mumbai, India). The bacterial strain *Pseudomonas elodea* NCIMB 12171 was procured from National Collection of Industrial, Food and Marine Bacteria (NCIMB), USA.

## Microorganism, culture maintenance, and inoculum preparation

*Pseudomonas elodea* NCIMB 12171 culture was maintained on slant prepared of yeast peptone glucose (YPG) agar medium (glucose 20 g/L, yeast extract 3 g/L, peptone 5 g/L, agar 15 g/L) as reported by Nampoothiri et al. (2003) and incubated at 37 °C for 36 h followed by storage at −4 °C. The inoculum was prepared by cultivating loop of cells in 50 mL sterile seed culture medium pH 7.0 (NaCl 5 g/L, yeast extract 1 g/L, peptone 5 g/L, beef extract 3 g/L, and sucrose 5 g/L) contained in 250 mL Erlenmeyer flask. The flasks were incubated at 250 rpm and 30 °C for 24 h in a rotary shaker.

## Chemical mutagenesis of the *Pseudomonas elodea* NCIMB 12171

The wild type *Pseudomonas elodea* NCIMB 12171 culture was subjected to mutagenesis using EMS as per the methodology reported by Cupples et al. (1990) with slight modifications. Briefly, 20 mL sterile seed medium was inoculated with loop of cells from the freshly sub-cultured plate. The inoculum was grown at 30 °C at 250 rpm for the next 16–20 h till suspension optical density (OD 600 nm) reached mid log phase. The suspension culture was harvested and centrifuged at 4000 × g followed by washing with 40 mL of phosphate buffer (100 mM; pH 7.0). The cell sediment was re-suspended in 5 mL phosphate buffer (100 mM; pH 7.0) and exposed to various concentrations of EMS (80, 160, 240, and 320 mM) at 30 °C for 60 min. Thereafter, the suspension was centrifuged at 4000 × g and double washed with 5 mL phosphate buffer. The cells were further suspended in 500 μL of same buffer and spread on sterile nutrient agar plates. Complete procedure was carried out in aseptic conditions. The plates were incubated at 30 °C until no distinct colonies were observed. The mutagenesis was targeted to have survival rate less than 1% which was confirmed using Eq. 1 as reported by Naveena et al. (2012) and Amraoui et al. (2022).

$$\text{Survival rate(\%)} = \frac{N_i - N_d}{N_i} * 100 \quad (1)$$

where  $N_i$  and  $N_d$  are the viable cell count, initially and after mutation in cfu/mL (colony forming unit/mL), respectively.

## Screening and characterization of mutant

The colonies survived were screened for their stability, morphology, and pigmentation by repeated passages on the nutrient agar plates. There were 28 colonies with consistent colony characteristics after 5 consecutive passages. All

of these were further evaluated for their ability to produce GG. The colony giving highest yield of GG (g/L) on alcohol precipitation of broth was selected for further study and hereafter named as “GGSM81.” It was checked for purity, shape, and motility under microscope and examined for Gram staining using K001-1KT (HiMedia, India).

The mutant GGSM81 was analyzed for 16S rRNA partial gene sequencing by extracting DNA as per the established protocol (Wilson 2001). The resulting 1257 bases so obtained were aligned with GeneBank database using BLAST server of NCBI for comparative assessment. neighbor-joining method was used to generate the phylogenetic tree. Similarly, it was also analyzed by MALDI Biotyper CA System (MBT-CA), Bruker Daltonics, Inc., Billerica, MA. The sample was prepared by direct transfer method as described by Faron et al. (2015). The isolate was deposited under Budapest Treaty at microbial depository of Microbial Type Culture Collection (MTCC), IMTECH, Chandigarh, India (Accession number: MTCC 25345).

## Submerged cultivation in shake flask

The submerged fermentation of the mutant GGSM81 for GG production was carried out in 500 mL Erlenmeyer flask containing 100 mL production medium. The production medium ( $K_2HPO_4$  1.5 g/L,  $KH_2PO_4$  1 g/L,  $MgSO_4 \cdot 7H_2O$  0.6 g/L, yeast extract 0.2 g/L, soy protein 2 g/L, and sucrose 30 g/L) was adjusted at pH 6 and autoclaved at 15 psig for 15 min. The sucrose solution was autoclaved separately and aseptically mixed with the production medium before inoculation. The production flasks were inoculated with 5% (v/v) and 20 h seed ( $6.45 \pm 0.5$  log cfu/mL) and were incubated at 30 °C for 52 h at 250 rpm in rotary shaker (Orbiteck; Scigenics Biotech, India).

## Optimization of cultivation conditions

The process parameters such as pH, temperature, and inoculum size were optimized by one factor at a time (OFAT) approach. The basic production media described in “Microorganism, culture maintenance and inoculum preparation” section was adjusted at pH 5, 6, 7, and 8 using 0.5 N HCL and 0.5 N NaOH before autoclaving. The sterile flasks were inoculated with 5% v/v inoculum of 20 h age ( $6.45 \pm 0.5$  log cfu/mL) and were incubated at 30 °C, 250 rpm for 52 h. Similarly, the effect of temperature on the production of GG was studied at 25, 30, 35, and 40 °C at optimum pH and 5% inoculum size. The optimum inoculum in terms of volumetric size (5%, 10%, 15%, and 20% v/v) with constant cell count ( $6.45 \pm 0.5$  log cfu/mL) was studied at optimum pH and temperature. All the experiments were performed in triplicate, and results were expressed as mean standard deviation.

## Optimization of the production medium by statistical design

The nutritional parameters were further optimized to maximize the production of GG by statistical design. Variables affecting the production of GG were screened by the Plackett–Burman design. The most influencing factors (sucrose, urea, and ADP) were then further optimized using response surface methodology. The level of sucrose, urea, and ADP was fixed based on their model coefficient and  $p$ -values after statistical analysis (please see supplementary file. Higher model coefficient (from 0.75 to 1.10) and lower  $p$ -values ( $p < 0.05$ ) of these factors were indicative of their positive influence on response, i.e., GG yield. This indicated that values higher than those tested through the Plackett–Burman design may further improve the response. Similarly, literature on fermentation for the production of microbial polysaccharides including GG also indicates that carbon source up to 4 to 6% w/v, urea up to 2.5 g/L, and ADP up to 1 mM is appropriate for higher yield (Bajaj et al. 2006; Bajaj et al. 2007; Huang et al. 2020; Prajapati et al. 2013; Dev et al. 2022). Hence, considering statistical analysis and literature reports, the levels of sucrose, urea, and ADP were fixed. All the submerged batch cultivations were performed in triplicate at optimized pH, temperature, and inoculum size in shake flasks. The results are presented as the average values of three trials.

## Production of gellan gum in a bioreactor

The batch cultivation of the mutant was done aseptically in 10 L stirred-tank bioreactor (BioFlo 120; Eppendorf, USA) with 7 L working volume. The 12 h polarized sterile vessel was inoculated with 10% (v/v) 20 h aged seed ( $6.45 \pm 0.5$  log cfu/mL). The inoculum was prepared as per procedure described in “[Microorganism, culture maintenance, and inoculum preparation](#)” section. The batch process was executed at 30 °C, and pH was maintained at  $7.0 \pm 0.5$  using 1N NaOH and 1N HCL. The foaming was controlled by automatic addition of silicon oil emulsion (GRM704, HiMedia, India). The samples were harvested and analyzed at every 4 h interval for cell growth, yield of GG, and residual sucrose concentration.

## Effect of dissolved oxygen

The yield of GG, cell growth, substrate consumption, and process productivity by the mutant *Sphingomonas trueperi* GGSM81 were studied with respect to variable dissolved oxygen tension (DOT) in bioreactor using optimized production media. The aeration and agitation were varied in the range of 300 to 600 rpm and 0.5 to 2.0 SLPM, respectively, to maintain DOT in the bioreactor at targeted levels of 20%, 40%, and 70%. Oxygen-enriched air was supplied as per demand beyond mentioned upper values of aeration and agitation. All the experiments were performed as batch process in triplicate, and results were recorded as mean  $\pm$  standard deviation.

Different kinetic parameters such as instantaneous growth rate ( $r_x$ ), instantaneous rate of product formation ( $r_p$ ), instantaneous rate of substrate consumption ( $r_s$ ), product formation specific rate ( $\mu_p$ ), substrate consumption specific rate ( $\mu_s$ ), and productivity ( $P_r$ ) were determined using equations discussed by Miranda et al. (2020).

## Kinetic modeling of gellan gum fermentation

Kinetic modeling of the fermentation process enables basic understanding about the cell growth and associated metabolic changes. Experimental values of cell count, residual sucrose, and gellan gum yield obtained from batch fermentation under optimized conditions were evaluated for different kinetic model fitting. Microbial hydrocolloid fermentation processes do not follow the classical substrate-limited cell growth and product formation kinetics. Hence, empirical models such as logistic equation are used as alternative to define the kinetics (Zhang et al. 2015). Like other polysaccharides, cell growth in GG fermentation process was modeled by logistic equation (Eq. 2)

$$\text{Logistic equation : } X_t = \frac{X_0 e^{\mu t}}{1 - \left(\frac{X_0}{X_t}\right)(1 - e^{\mu t})} \quad (2)$$

where  $X_t$  = cell growth at time “t” [log (cfu/mL)],  $X_0$  = cell count at beginning,  $\mu$  = specific growth rate ( $\text{h}^{-1}$ ), and  $t$  = time (h). The product formation was modeled by Luedeking–Piret model (Eq. 3).

$$\text{Luedeking – Piret model : } P_t = P_0 + \alpha X_0 \left( \frac{e^{\mu t}}{1 - \left(\frac{X_0}{X_m}\right)(1 - e^{\mu t})} - 1 \right) + \beta \frac{X_m}{\mu m} \ln \left( 1 - \frac{X_0}{X_m} (1 - e^{\mu t}) \right) \quad (3)$$



The kinetics of substrate consumption was modeled by Weibull model (Eq. 4) and exponential decay model (Eq. 5).

$$\text{Weibull model : } \text{Log}(S_t) = -\mu t^n \quad (4)$$

$$\text{Exponential decay model : } S_t = S_0 e^{-\lambda t} \quad (5)$$

## Analytical methods

### Cell count and gellan gum quantification

Cell count in the fermentation broth samples was determined by streak plate method. Briefly, broth was serially diluted in the saline solution to make  $10^{-1}$  to  $10^{-5}$  dilutions and plated on the sterilized MS agar plate in triplicate followed by incubation at 30 °C for 24–48 h. The cell count was expressed as average of three plate counts. The GG from the fermentation broth was quantified by alcohol precipitation as reported by Bajaj et al. (2006).

### Physico-chemical characterization of the gellan gum

#### Compositional analysis by HPLC

The samples were hydrolyzed using 2 M trifluoroacetic acid (TFA) at 90 °C for 3 h. The residues were washed with HPLC grade methanol repeatedly for 2–3 times by evaporating the methanol to dryness in order to remove the acid component. The dried residue was dissolved in HPLC grade water and filtered through 0.22  $\mu$  PVDF filters. The samples were loaded on the COSMOSIL Sugar-D packed column (4.6 ID  $\times$  500 mm, 05397–51) and analyzed using RI-4070 refractive index detector (RID) HPLC system (JASCO, Japan). The analyses were done at a column temperature of 40 °C using acetonitrile: water (70:30) as the mobile phase in isocratic elution mode at 1 mL/min flow rate. The commercial gellan gum Clerigel was used as control.

#### Determination of acetyl content

The acetyl content was determined by colorimetric method as described earlier (Hestrin 1949). Briefly, 2 mL of alkaline hydroxylamine reagent was added to 1 mL sample (100  $\mu$ g/mL). The solution pH was adjusted at  $1.2 \pm 0.2$  using 1N HCl. The chromogenic solution of ferric chloride (1 mL) was added into the mixture and shaken gently. The absorbance was measured using UV–Vis spectrophotometer at 540 nm (SpectroStar microplate reader, BMG Labtech, Germany). The blank was prepared using distilled water instead of sample. Standard curve was prepared using acetylcholine chloride (45–3600  $\mu$ g/mL) solutions (0.004 M, in

0.001 N; pH 4.5 sodium acetate solution). Standard curve has been provided in the supplementary file (SI F1).

### Other physico-chemical properties

The other physico-chemical properties such as ash content and protein content were determined following the methods reported in Association of Official Analytical Chemist (AOAC 2005). The color values such as  $L^*$ ,  $a^*$ , and  $b^*$  were determined using Hunter Lab colorimeter (LabScan XE, Hunter Associates Laboratory, VA, USA) with standard settings (D65/10°, reflection mode). The water activity ( $a_w$ ) was measured using RotoMac™ at  $25 \pm 1$  °C.

### Structural characterization

#### FTIR

The test samples and Clerigel were analyzed for functional groups using ATR-FTIR of Alpha Instruments, Bruker, USA. The samples were scanned for 4000–400  $\text{cm}^{-1}$  frequencies at 4  $\text{cm}^{-1}$  resolution.

#### NMR

Polysaccharide from mutant GGSM81 and Clerigel was analyzed by  $^1\text{H}$ -NMR. The samples were prepared at concentration 5 mg/mL in  $\text{D}_2\text{O}$  and analyzed at 90 °C using 600 MHz NMR, JEOL, Japan, at 14 T filed strength, 2.75 Hz resolution, and 11.28 kHz frequency sweep.

#### Molecular weight

The GG from mutant GGSM81 was evaluated for the molecular weight by gel permeation chromatography (GPC) and compared with the commercial gellan gum, Clerigel for their number average molecular weight, weight average molecular weight, and molecular weight distribution. The solution (0.5 mg/mL) was prepared in deionized water by overnight hydration. The samples were injected on PL Aquagel OH-40 column through guard column at a flow rate of 1 mL/min and analyzed by refractive index detector (RID) of Agilent 1260 multi-detector system. For every analysis, calibration curve was plotted using range of known molecular weight dextran (668–5.2 kDa).

#### Thermal characterization

The commercial GG and GG from mutant GGSM81 were analyzed for their thermal properties using differential scanning calorimetric, Shimadzu, Japan. The analysis

was carried out under nitrogen ( $N_2$ ) flow for thermal cycle from 25 to 500 °C at 10 °C/min. The results were processed using TA software (TA instruments, New Castle, DE, USA). TGA measurements of Clerigel and GG from mutant GGSM81 were performed in nitrogen flow (100 mL/min) in a temperature range of 25 to 500 C at 10 °C/ min in TA instrument.

### Microscopic analysis

The microstructural characteristics of the powdered GG and commercial Clerigel were studied by Scanning Electron Microscopy (SEM) using Quanta 200F ESEM (FEI Company, Netherland) with accelerating voltage of 20.0 kV under low vacuum condition.

### Rheological analysis

The rheological characterization of GG solution was performed using MCR-e302 rheometer (Anton Paar, Austria) equipped with parallel plate geometry (0.5 mm gap, PP50). The analysis was performed at 25 °C. The equilibrated sample was analyzed for flow curve parameters such as shear stress ( $\sigma$ ), apparent viscosity ( $\eta_a$ ), and over shear rate ( $\dot{\gamma}$ ) 0.1 to 100  $s^{-1}$ . The data was used to determine flow behavior index ( $n$ ), consistency index ( $k$ ), and yield stress. Similarly, the frequency test was determined in frequency 0.01 – 10 rad/s with shear strain 1%.

### Statistical analysis

All the experiments were performed in triplicate. The statistical significance of the experimental observations has been performed by analysis of variance (ANOVA), followed by

Duncan's multiple range test for multiple comparisons using the IBM®, SPSS® statistics software (version 20) (NY, USA) at  $p < 0.05$  significance level.

## Results and discussion

### Mutant generation, selection, and characterization

The random mutagenesis by any physical or chemical methods is well known to produce microbial strains with superior characteristics. These techniques alter the genetics of the wild microorganism either by in vivo addition or deletion of the nucleotides (Foster 1991). EMS as chemical mutagen works by irreversible alterations in the base sequence of DNA or by creating a lesion in the DNA sequence. The ethyl group from EMS owes its overall mutagenic capacity. This ethyl group transfers to available nucleophilic sites, principally nitrogen, but it could also be at oxygen or phosphate group in the DNA (Bleisch et al. 2022; Segal 1984). The transfer occurs via  $SN_1/SN_2$  reaction mechanism which immediately tends to be corrected by the molecular assembly of the microorganism. However, microorganisms which are not able to correct such alterations or lesions and still survive on the nutrient supplements are termed as mutants (Segal 1984; Devchand and Gwynne 1991; Amraoui et al. 2022; Bleisch et al. 2022). In the present study, EMS treatment was observed to have lower survival rate at higher EMS concentration (Fig. 1a).

Among the survived colonies, only 28 mutants were stable on passaging which were then screened for their colony characteristics and GG yield. Among these, GGSM81 mutant consistently gives large, mucoid, convex, and slightly yellow-colored colonies and shortlisted for further study. It was observed to be aerobic, rod-shaped, non-spore forming

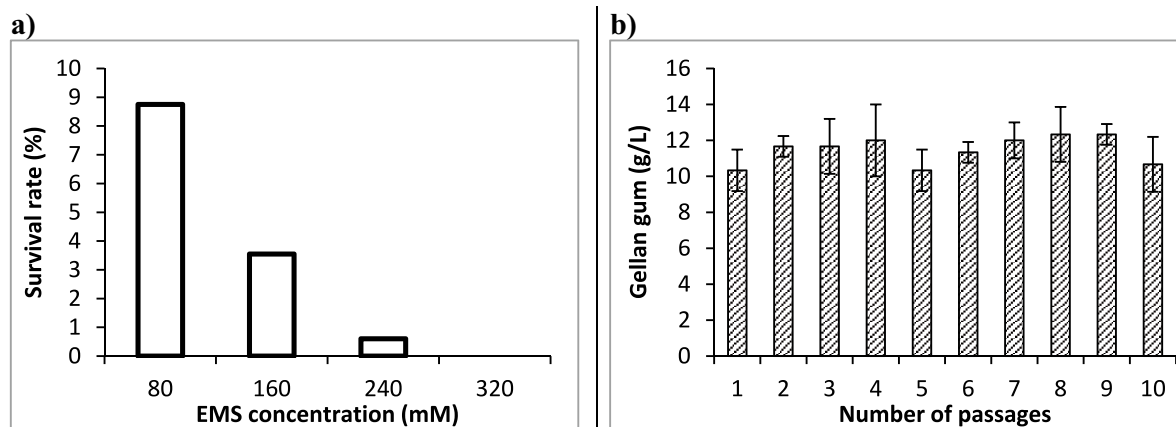
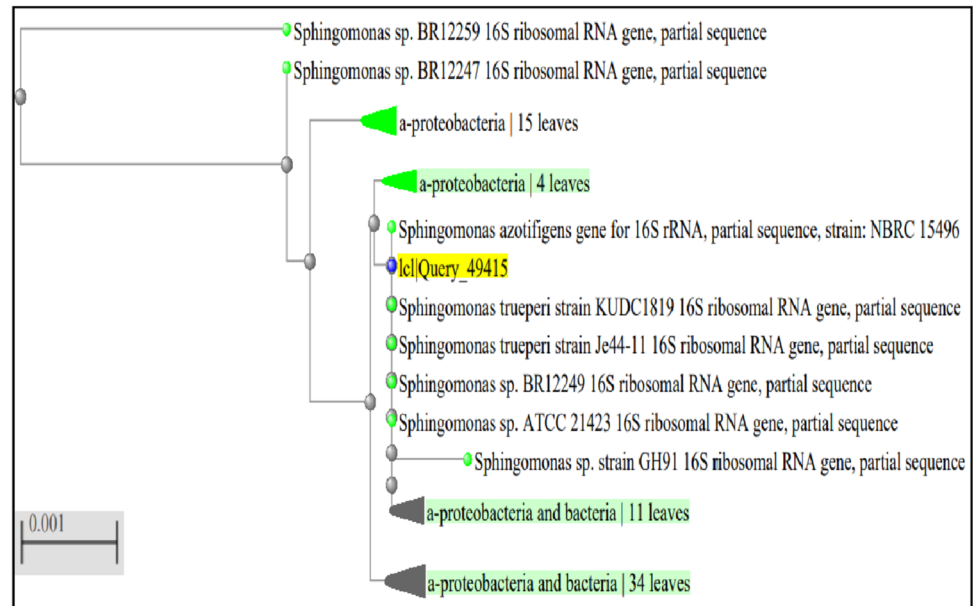


**Fig. 1** a Survival rate of *Pseudomonas elodea* NCIMB 12417 against different EMS concentration. b Generation stability of mutant *Spingomonas trueperi* GGSM81 for gellan production

**Fig. 2** Phylogenetic tree showing close relationship of mutant GGSM81 with other species based on neighbor-joining method



Gram negative in character showing consistent GG yield (10–13 g/L) over 10 production cycles with similar colony characteristics (Fig. 1b). The yield (g/L) and productivity (g/L/h) were much higher than the wild type strain producing GG up to 6–7 g/L after 96 h of shake flask fermentation. Li et al. (2019) have reported 14.4% increment in GG yield from mutant *Sphingomonas* spp. after combined UV and EMS treatment on wild *Sphingomonas elodea*. Lobas et al. (1992) also have reported four-fold increased in GG productivity by *Sphingomonas paucimobilis* E2 (DSM 6314) which was a mutant of an industrial strain *Auromonas elodea* (ATCC 31461) developed using EMS as mutagen. Similarly, increased xanthan gum production in *Xanthomonas campestris*, EPS production in *Cordyceps militaris* SU5-08, and pullulan production in *Aureobasidium pullulan* have been reported after random mutational breeding (Lin et al. 2012; Kothari et al. 2014; Li et al. 2023).

Based on 16S rRNA analysis, phylogenetically mutant GGSM81 showed 100% similarity with *Sphingomonas trueperi* KUDC1819 (partial sequence, query covered = 100%, E. value: 0.0, Accession number: KC3553261.1), *S. trueperi* Je44-11 (partial sequence, query covered = 100%, E. value: 0.0, Accession number: KC152652.1), 99.92% similarity with *S. trueperi* NBRC 100456 (partial sequence, query covered = 100%, E. value: 0.0, Accession number: NR\_113897.1), and 99.76% similarity with *Sphingomonas azotifigens* BT364 (partial sequence, query covered = 100%, E. value: 0.0, Accession number: MN204209.1). Phylogenetically mutant GGSM81 were closer to *S. trueperi* followed by *S. azotifigens* with 14 and 12 number of hits during nucleotide BLAST, respectively (Fig. 2). Similarly, MALDI-TOF mass spectroscopic analysis also confirmed the mutant closeness with *S. trueperi*. It has been deposited in Microbial Type Culture Collection (MTCC), Chandigarh

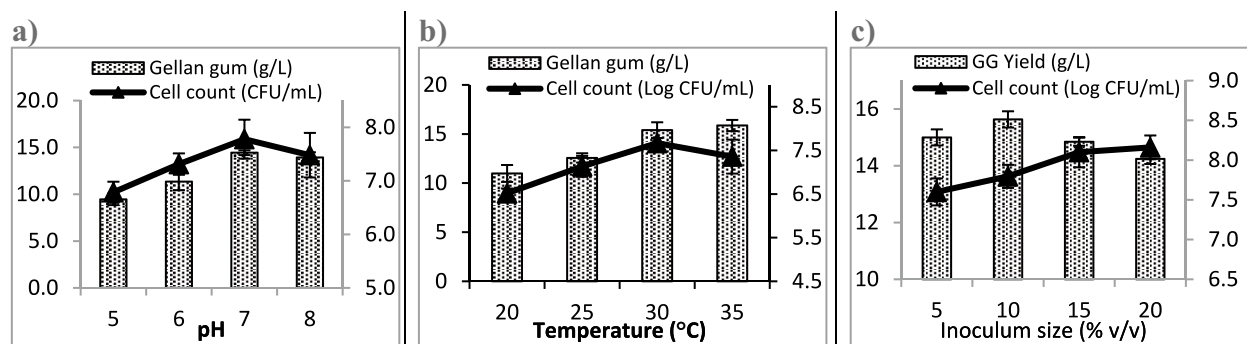


**Fig. 3** Effect of process parameters on the cell growth and yield of gellan gum by mutant *Sphingomonas trueperi* GGSM81: **a** pH, **b** temperature, and **c** inoculum size

depository under Budapest Treaty with accession number MTCC 25345. Considering the high GG production capacity, mutant GGSM81 was used to optimize fermentation conditions aiming for maximum yield and productivity.

## Optimization of culture conditions

### Effect of pH on the gellan gum yield

The effect of pH on the yield of GG by the mutant strain GGSM81 is depicted in Fig. 3a. The bioprocess pH is a decisive parameter for nutrient solubility, cellular physiology, and hence the overall metabolism. In the present study, maximum GG yield (14.4 g/L) was observed at pH 7 beyond which it declined. This indicated a reduced cell growth in alkaline environment and consequently decreased product formation (Nampoothiri et al. 2003; Bajaj et al. 2006). The optimum pH for growth and production may vary for the same bacterium. Our results are in agreement with literature reports (Bajaj et al. 2007; Raghunandan et al. 2018). However, few reports suggest that acidic stress (pH 5 to 6.5) boosts the exopolysaccharide production, but it specifically varies for individual bacterial strain (Sengupta et al. 2018; Dev et al. 2022).

### Effect of temperature on the gellan gum yield

Figure 3b depicts the effect of temperature on the yield of GG. An increase in temperature increased the yield of GG with maximum yield (15.9 g/L) being obtained at 35 °C. However, there was non-significant difference between GG yield at 30 and 35 °C. Temperature influences the physiological and biochemical characteristics of the bacteria by directing role of multiple enzymes in metabolic pathways and hence the rate of biochemical reactions (Dev et al. 2022). Therefore, higher temperature is known to promote the secretion of shorter chains of GG (Martins and Sá-Correia 1994). The results are in agreement with the literature reporting 30 °C as optimal temperature in GG fermentation (Kamer et al. 2021; Dev et al. 2022).

### Effect of inoculum size on the gellan gum yield

Inoculum size determines the extent of the lag phase in the batch profile, overall growth pattern, and GG biosynthesis. An inoculum of 10% v/v was observed to produce maximum yield of GG (15.6 ± 0.3 g/L) which was slightly higher than GG yield at 15% v/v inoculum size (14.8 ± 0.6 g/L). Comparatively lower GG yield (14.3 ± 0.4) was observed at 20% v/v inoculum size (Fig. 3c). This decrease in GG production with increasing inoculum size could be due to increasing cell population density. The cell density at the beginning of batch in 5, 10, 15, and 20% v/v inoculum was 5.1, 5.5, 5.7, and 5.8 log cfu/mL (see supplementary file) which ultimately led to

the production of more biomass with progress in fermentation (Fig. 3c). Such high cell density obviously utilizes more substrate for growth and proliferation as compared to lower cell density system (Bajaj et al. 2007; Prajapati et al. 2013). The results are in agreement with the literature reporting 10 to 15% v/v inoculum size as optimum for GG bioprocessing in batch fermentation (Bajaj et al. 2007; Sukumar et al. 2021; Dev et al. 2022).

## Optimization of the production medium by statistical designs

### Plackett–Burman design

In the Plackett–Burman design, eleven factors were assessed through 12 different trials giving variable GG yield from 6.8 to 13.9 g/L for different runs. The correlation coefficient ( $r$ ) of the model was 0.9573, indicating a good agreement between the experimental data and the model-predicted values. The determination coefficient ( $R^2 = 0.9884$ ) indicated that nearly 99% of the variation in gellan gum yield could be attributed to the experimental factors (see supplementary file).

Based on the model coefficient and  $p$ -value, sucrose, urea, and ADP were observed to prominently affect the GG yield (see supplementary file). Sucrose is one of the major carbon supplements in the environment. Most of eubacteria including *Sphingomonas* spp. possess sucrose catalyzing enzymes, i.e., sucrose-6-phosphate hydrolases and sucrose phosphorylases. These enzymes empower the metabolism of this disaccharide in a controlled fashion to glucose-6-phosphate and fructose-6-phosphate through phosphotransferase system (PTS) and/or non-PTS permease transport system to make it easily available for different glycolytic pathways (Reid & Abratt 2005). This has been evident by utilization of sucrose as prominent carbon source in the production of GG (Arockiasamy and Banik 2008; Wang et al. 2020; Dev et al. 2022). Similarly, nitrogen is a key element of the cellular metabolism for the synthesis of amino acids, proteins, nucleic acids, enzymes, and key energy buckets including ADP and ATP. However, preferential utilization of different nitrogen sources is strain dependent. *S. paucimobilis* ATCC 31461 utilizes organic nitrogen such as peptone, yeast extract, and tryptone, whereas strain-like *S. paucimobilis* GS1 and *S. azotifigens* GL-1 utilize inorganic nitrogen from potassium nitrate and ammonium chloride, respectively (Wang et al. 2020). Model statistical analysis (ANOVA) indicates preferential use of inorganic nitrogen from urea by mutant *S. trueperi* than other organic nitrogen sources screened (see supplementary file). Similarly, higher linear coefficient for ADP indicates its positive influence on GG production (see supplementary file). This could be due to its role as energy source for various biochemical reactions as well as precursor in GG biosynthesis (Bajaj et al. 2006; Dev et al. 2022). These



**Table 1** Central composite design for optimization of media components for the production of gellan gum by *Sphingomonas trueperi* GGSM81

Run	Sucrose (g/L)	Urea (g/L)	ADP (mM)	Gellan gum yield (g/L)	
				Actual value <sup>a</sup>	Predicted value
1	35	1.5	1.00	15.9±0.35	15.8
2	35	3.0	1.00	14.0±0.60	14.2
3	35	1.5	2.00	13.5±0.25	13.4
4	35	3.0	2.00	11.8±0.42	11.8
5	70	1.5	1.00	21.0±0.70	20.4
6	70	3.0	1.00	14.4±0.55	13.9
<b>7</b>	<b>70</b>	<b>1.5</b>	<b>2.00</b>	<b>21.6±0.65</b>	<b>20.8</b>
8	70	3.0	2.00	14.9±0.40	14.3
9	52.5	0.99	1.50	12.9±0.75	13.5
10	52.5	3.51	1.50	6.42±0.30	6.7
11	52.5	2.25	0.66	19.3±0.55	19.7
12	52.5	2.25	2.34	17.3±0.67	17.9
13	23.1	2.25	1.50	14.9±0.28	14.7
14	81.9	2.25	1.50	19.5±0.91	20.7
15	52.5	2.25	1.50	13.2±0.64	15.1
16	52.5	2.25	1.50	16.0±0.81	15.1
17	52.5	2.25	1.50	15.5±0.85	15.1
18	52.5	2.25	1.50	15.1±0.78	15.1
19	52.5	2.25	1.50	15.8±0.90	15.1
20	52.5	2.25	1.50	14.9±0.72	15.1

<sup>a</sup>Values are mean ± SD of three or more determinations; The bold values indicate the combination of experimental variables for highest GG titer

factors were further optimized for their optimum numerical values by response surface methodology (RSM).

### Response surface methodology (RSM)

A total 20 runs were carried out, and their predicted and experimental values of GG yield as response are shown in Table 1. The overall quadratic modeling showed good fitting with  $p$ -value less than 0.0001, model  $F$ -value (25.14), and determination coefficient ( $R^2=0.9577$ ) that suggested statistical significance of the model (see supplementary file). As per the statistical analysis of model, concentrations of sucrose and urea as well as its interaction effects had significant coefficients ( $p < 0.05$ ). Surprisingly, contrary to the Plackett–Burman results, negative coefficients (linear and interaction) showed that an increase in the urea concentration decreased the yield of GG. A possible reason for such observation could be a change in the C/N ratio as well as change in organic to inorganic nitrogen ratio which is reported to navigate the GG production in *Sphingomonas* spp. (Kanari et al. 2002; Huang et al. 2012; Wang et al. 2020). Similarly, higher inorganic nitrogen concentration is reported to improve the cell growth/biomass but limits the GG production (Bajaj et al. 2006; Dev et al. 2022) as well as the concentration of type and concentration of nitrogen source directs the flow of carbon source towards either

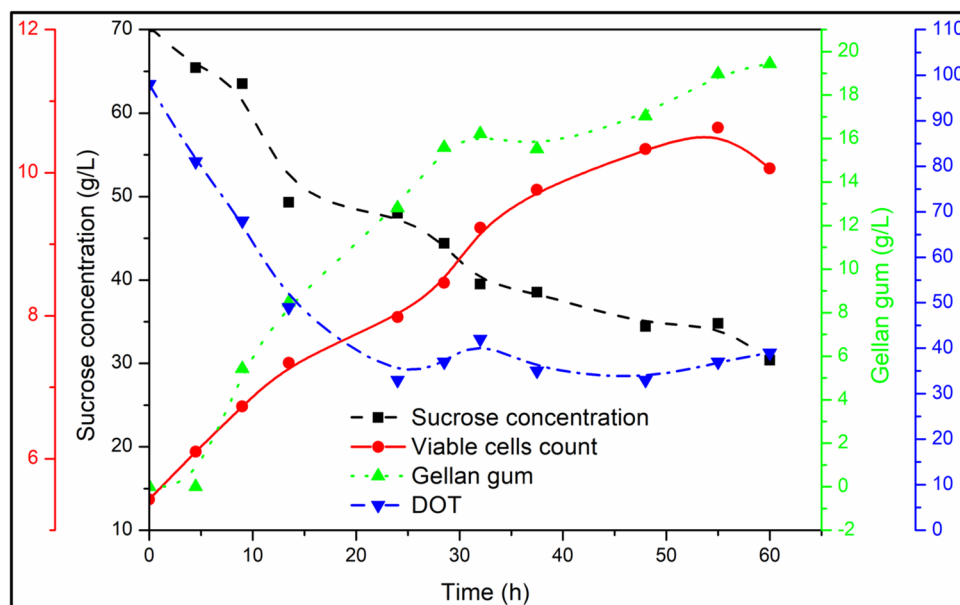
biomass or GG formation (Ashtaputre and Shah 1995; Wang et al. 2020). Contrary to this, inorganic nitrogen such as urea is reported to be efficiently used at concentration 2.5 g/L by *Sphingomonas* spp. for growth and GG production (Huang et al. 2020). Moreover, interaction of ADP and sucrose concentration in their additive terms showed irrelevance on the yield of GG (see supplementary file). The higher amount of energy associated with the phosphate bonds of ADP are used in the cellular synthesis of primary and secondary metabolites. Similarly, activated precursors of nucleotide phosphate sugars such as ADP are reported to be required in the GG biosynthesis (Kanari et al. 2002) and reported to influence the carbon utilization (Bajaj et al. 2006). The results are in agreement with the literature claiming C/N ratio and presence of precursors to dictate the fermentation yield of GG (Fialho et al. 2008; Prajapati et al. 2013; Dev et al. 2022).

### Production of gellan gum production in bioreactor

Figure 4 depicts the fermentation batch profile of the mutant *Sphingomonas trueperi* GGSM81 using the RSM-optimized medium in a 10 L bioreactor.

It suggested the growth dependent production of GG in the exponential phase. The production profiling also suggested cell death in the stationary phase which could be due to high viscosity limiting mass transfer. The pH of broth

**Fig. 4** Fermentation profile of the mutant *Sphingomonas trueperi* GGSM81 in optimized medium



dropped from 7.0 to 5.2 during batch fermentation, which demonstrated active cell metabolism producing acidic intermediates during GG biosynthesis (observed when performed batch fermentation with pH uncontrolled mode under identical process conditions). A consistent decrease in DOT from the lag phase to stationary phase was observed attaining 30% saturation level after 24 to 26 h of fermentation. It was maintained above 30% onwards by means of agitation (gradually increasing from 300 to 600 rpm), aeration (gradually increasing from 0.5 to 2.0 SLPM), and by gradual increased in oxygen supply by increasing its fraction in sterile air (from 0 to 50%) as per demand. The GG production was seen to increase consistently during whole batch fermentation with highest yield of 19.4 g/L at 62 h. This suggested that lower DOT saturation improves the yield of GG. The results are in agreement with the literature affirming low DOT as stimuli for GG biosynthesis (Giavasis et al. 2006; Huang et al. 2012; Dev et al. 2022).

### Effect of dissolved oxygen tension

Effect of DOT on the fermentation batch profile was studied at 20, 40, and 70% DOT. It was observed that the DOT greatly influenced the batch fermentation profile of the mutant *Sphingomonas trueperi* GGSM81. Bioreactor under low DOT promoted the production of GG and also improved the kinetics of cell growth, substrate utilization, and product formation (Fig. 5 and Table 2).

A decrease in DOT from 70 to 20% increased the yield of GG from  $15 \pm 1.3$  to  $23 \pm 2.4$  g/L with approximately 2.5-fold-improved productivity from 0.29 to 0.51 g/L/h. These observations are accordance with the reports by Giavasis et al. (2006) after detailed investigation of aeration

and agitation effect on GG fermentation. The batch yield ( $23 \pm 2.4$  g/L) of GG and productivity from mutant GGSM81 was observed to be competitive with reported values in literature (Table 3) (Dev et al. 2022). Furthermore, there is a scope for investigation of various approaches such as feeding rate of carbon or nitrogen source, fed-batch fermentation, and use of inducers such as hydrogen peroxide to enhance overall productivity (Wang et al. 2006; Zhang et al. 2015; Dev et al. 2022).

Figure 5d depicts the effect of GG concentration in the broth on the rate of gellan production. It was clearly seen that DOT non-significantly influenced the rate of GG production with initial values of 0.48, 0.59, and 0.68 g/L/h for 70, 40, and 20% DOT, respectively. However, the rate of gellan production decreased beyond 7 to 8 g/L gellan concentration in the broth. This must be due to viscosity contribution by GG, limiting the mass and oxygen transfer in the broth. Similar observations have been reported by Arockiasamy and Banik (2008). A significant decrease in the cell count between 35 and 45 h of fermentation at all tested DOT could be due to high viscosity of the broth which limited the efficient nutrient transfer and ultimately leading to autolytic cell death (Giavasis et al. 2000). An extensive lag phase was observed at high DOT promoting the cell growth, whereas at low DOT, a short lag phase brought about an early exponential phase. This indicates higher rate of instantaneous cell growth and instantaneous product formation as indicated in Table 2.

### Kinetic modeling of gellan gum fermentation

Figure 6 depicts the kinetics of cell growth, substrate utilization, and product formation of GG.

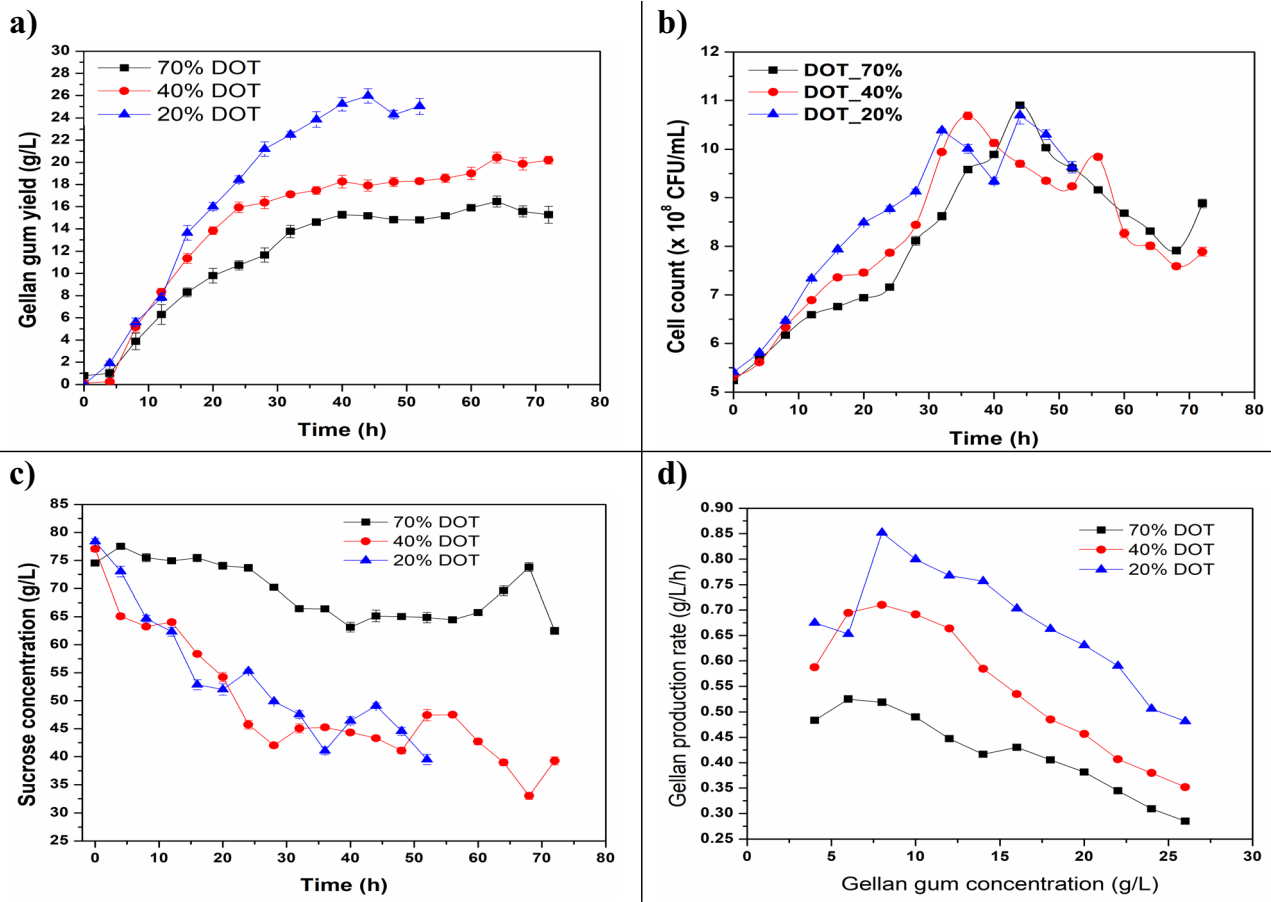


**Fig. 5** Effect of dissolved oxygen tension (DOT) on batch fermentation profiling of gellan gum by *Sphingomonas trueperi* GGSM81: **a** gellan gum yield, **b** cell count, **c** substrate consumption, and **d** effect of gellan gum broth concentration on its production

**Table 2** Effect of dissolved oxygen tension (DOT) on the expressions of kinetic parameters, yield of gellan gum, and batch productivity by *Sphingomonas trueperi* GGSM81

Dissolved oxygen tension							
70%							
Kinetic parameter	$r_x$	$r_p$	$r_s$	$\mu_x$	$\mu_s$	$\mu_p$	$P_r$
12 h	1.59	0.53	3.12	0.58	0.34	0.03	0.46
24 h	0.84	0.45	1.53	0.39	0.15	0.02	0.42
36 h	0.60	0.41	0.92	0.36	0.09	0.02	0.38
48 h	0.46	0.31	0.68	0.29	0.06	0.01	0.29
40%							
12 h	1.58	0.69	2.67	0.55	0.28	0.03	0.69
24 h	0.88	0.66	0.95	0.48	0.09	0.03	0.66
36 h	0.70	0.49	0.63	0.58	0.05	0.02	0.48
48 h	0.46	0.38	0.43	0.29	0.04	0.02	0.38
20%							
12 h	1.65	0.65	2.60	0.72	0.26	0.04	0.65
24 h	0.98	0.77	1.15	0.71	0.10	0.03	0.77
36 h	0.70	0.66	0.57	0.58	0.05	0.03	0.66
48 h	0.54	0.51	0.46	0.47	0.04	0.02	0.51

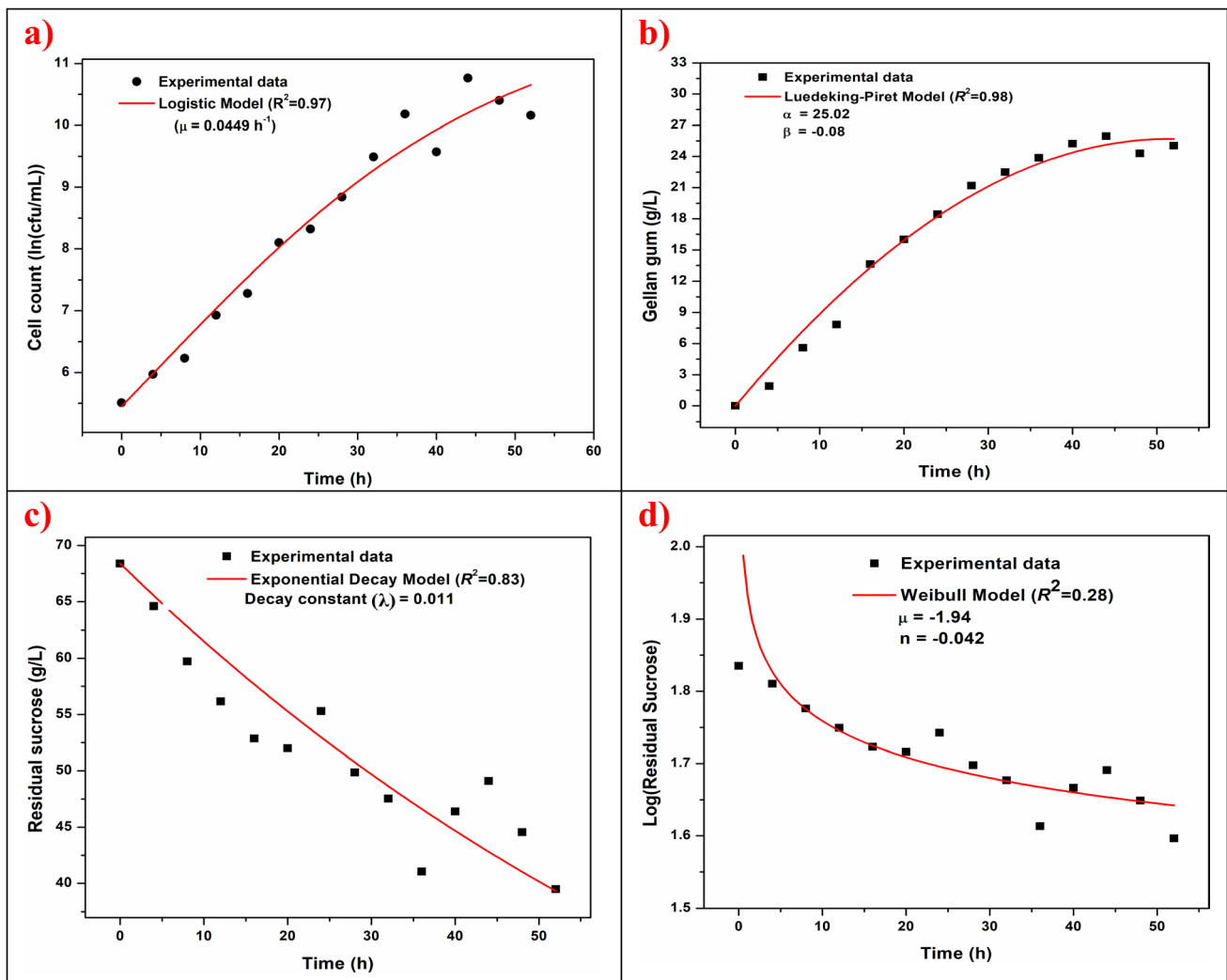
$r_x$ , cell growth instantaneous rate (g/L/h);  $r_p$ , product formation instantaneous rate (g/L/h);  $r_s$ , substrate consumption instantaneous rate (g/L/h);  $\mu_x$ , cell growth specific rate ( $\text{h}^{-1}$ );  $\mu_p$ , product formation specific rate ( $\text{h}^{-1}$ );  $\mu_s$ , substrate consumption specific rate ( $\text{h}^{-1}$ );  $P_r$ , productivity (g/L/h)

**Table 3** Experimental and literature values of batch fermentation process outcomes

Carbon source	Concentration (g/L)	GG titer (g/L)	Productivity (g/L/h)	References
Glucose	30	8.72	0.18	Lobas et al. 1992
Glucose	30	14.75	0.25	Wang et al. 2006
Sucrose	40	27.86	0.58	Arockiasamy and Banik 2008
Glucose	30	15.7	0.39	Huang et al. 2012
Waste glycerol	80	52.6	0.31	Raghunandan et al. 2018
Cheese whey	68	33.75	0.70	Wang et al. 2020
Grape pomace	50	12.08	0.17	Kamer et al. 2021
Sucrose	70	23.4	0.51	Present study

The logistic model was used to express the cell growth by taking  $X_0 = 5.45 \log$  (cfu/mL) and  $X_m = 10.8 \log$  (cfu/mL). The model showed a good fit between experimental values and model-predicted values for the cell

growth data ( $R^2 = 0.97$ ) with maximum specific cell growth rate of  $0.05 \text{ h}^{-1}$  (Fig. 6a). The statistical analysis (ANOVA) showed higher  $F$ -value (1009) and lower  $p$ -value ( $p < 0.05$ ) assuring the ability of model to predict

**Fig. 6** Kinetic modeling of growth, sucrose consumption, and gellan production by *Sphingomonas trueperi* GGSM81

the experimental values. The results are in agreement with the literature reporting logistic model as best fit to describe cell growth during the production of GG and other similar polysaccharides (Wang et al. 2006; Dev et al. 2022). As depicted in Fig. 6c, d, exponential decay model ( $R^2=0.83$ ) provided good fit for substrate utilization over Weibull model ( $R^2=0.28$ ). It has been confirmed by higher model  $F$ -value for exponential decay model ( $F$ -value = 3246) than Weibull model ( $F$ -value = 66.6). The model predicted and experimental values of GG production were observed to best fitted with Luedeking-Piret model with correlation coefficient 0.98 (Fig. 6b). The result suggests linear correlation between GG production and cell growth (Mitra and Dutta 2018). The higher value of “ $\alpha$ ” ( $> 1$ ) and lower value of “ $\beta$ ” ( $< 0$ ) cumulatively indicate the growth-associated GG formation. The results are also in agreement with literature reporting higher  $\alpha$  value and lower  $\beta$  value for the production of GG in batch fermentation (Wang et al. 2006).

### Physico-chemical characterization of gellan gum

The HPLC analysis of the polysaccharide from *Sphingomonas trueperi* GGSM81 confirmed the glucose, rhamnose and glucuronic acid as its constituents (see supplementary file), which is line with the commercial GG. The hydrocolloid obtained from mutant *Sphingomonas* spp. was with high degree of acylation (5.9%) compared with the Clerigel (0.5%). There was significant difference between the ash and protein content as well as color values ( $L^*$ ,  $a^*$ ,  $b^*$ ) and water activity ( $a_w$ ) (Table 4, part a). This could be due to variation in the strain, culture medium or culture conditions, deacylation treatment, and downstream processing as widely reported in the literature (Prajapati et al. 2013; Kamer et al. 2021). However, it indicates the scope for optimizing the downstream operations.

### Structural characterization

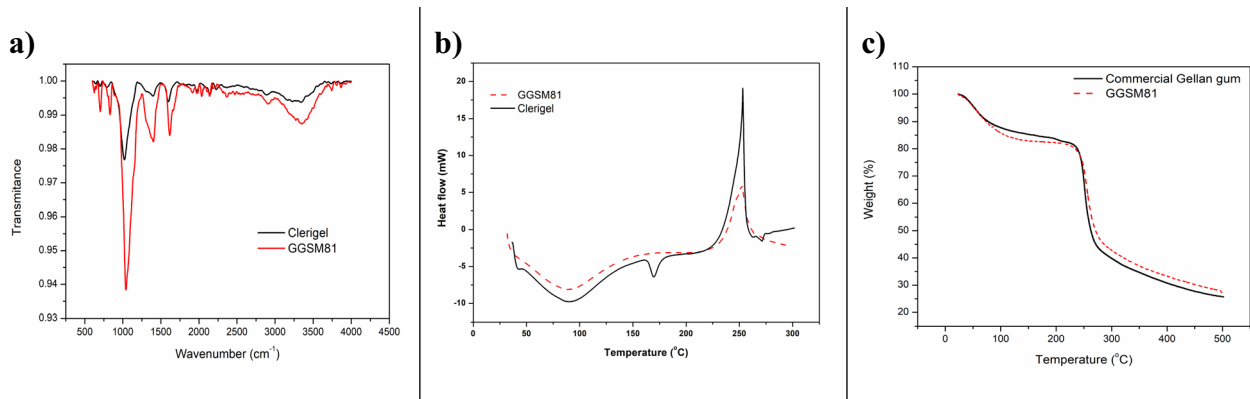
#### FTIR

Figure 7a depicts the spectral pattern for commercial GG and the GG produced by the mutant GGSM81. For both the samples, the major absorption was recorded at  $\sim 3400$ – $3300\text{ cm}^{-1}$ ,  $3000$ – $2850\text{ cm}^{-1}$ ,  $1620$ – $1550\text{ cm}^{-1}$ ,  $1410$ – $1300\text{ cm}^{-1}$ , and  $1300$ – $1000\text{ cm}^{-1}$  which could be attributed for polymeric hydroxyl group stretching, -C-H stretching of methyl group, carboxylic acid or carboxylic acid ionic salt, tertiary alcohol and last for primary or secondary alcohol, or -C=O stretch of ester group, respectively. Similarly, the peak in the region  $1620$ – $1550\text{ cm}^{-1}$  reflected the presence of glycosidic linkage in the molecule. The results are in good

**Table 4** Evaluation of commercial gellan gum and that produced by *Sphingomonas trueperi* GGSM81 for (a) physico-chemical properties, (b) proton (1H) NMR peak analysis, and (c) flow behavior and dynamic rheology

(a) Physico-chemical and color analysis of Clerigel and GG from mutant GGSM81						
Sample	Protein content (% N)	Ash content (% w/w)	Water activity ( $a_w$ )	$L^*$	$a^*$	$b^*$
Clerigel	0.98 ± 0.24	5.24 ± 0.11	0.298 ± 0.006	88.8 ± 0.01	-0.41 ± 0.01	6.94 ± 0.0.01
GGSM81	2.34 ± 0.38	12.16 ± 0.79	0.514 ± 0.003	66.7 ± 0.03	1.11 ± 0.01	9.49 ± 0.01
(b) Proton NMR peak profile Clerigel and GG from mutant GGSM81						
Proton chemistry	Clerigel	GGSM81				
-CH of rhamnose	5.59					
-CH- of glucose	5.38					
-CH- of glucuronic acid	5.15					
-CH <sub>3</sub> - of rhamnose	1.80					
(c) Flow behavior of Clerigel and GG from mutant GGSM81						
Sample	Consistency index (K)	Flow behavior index (n)	Yield stress ( $\sigma_0$ )	Apparent viscosity ( $\eta$ )		
Clerigel	1.18 ± 0.05	0.47 ± 0.01	9.72	118.09 ± 1.44		
GGSM81	0.43 ± 0.04	0.46 ± 0.01	4.86	80.64 ± 2.02		





**Fig. 7** Characterization of Clerigel and gellan gum from *Sphingomonas trueperi* GGSM81 by **a** FTIR and thermal analysis by **b** DSC and **c** TGA

agreement with reported literature on GG (Sudhamani et al. 2003; Dev et al. 2023).

### NMR

The proton NMR spectra of GG obtained from GGSM81 as well as Clerigel showed all the characteristic peaks of structural arrangements reported for GG (Coutinho et al. 2010) (Table 4, part b). The sample from mutant GGSM81 also showed an extra high intensity peak at  $\delta$  2.65 ppm and  $\delta$  3.57 ppm which corresponded to the acetyl group (please see supplementary file). Similar observations have also been reported by Coelho et al. (2019). The low resolution and some interference in the GGSM81 sample around  $\delta$  2.45 ppm could be due to presence of impurity such as yeast extract in the sample (Osmalek et al. 2014; Coelho et al. 2019).

### Molecular weight

The molecular weight of GG varies from few hundred to thousand kilodaltons which offers different rheological and other functional properties (Hamcerencu et al. 2008; Coutinho et al. 2010). The entire tested sample including standard showed a mixture of GG of varying molecular weights (please see supplementary file). The GG from GGSM81 had a higher molecular weight and number average molecular weight of 2,531,733 and 2,046,225 g/mole than commercial GG which had corresponding values of 1,103,157 and 604,537 g/mole, respectively. The results are in good agreement with literature reporting variable range of GG from different sources (Hamcerencu et al. 2008; Coutinho et al. 2010).

### Thermal analysis

The thermal properties such as DSC and TGA of GG from mutant GGSM81 were studied and compared with

commercial sample. The DSC thermogram of both the samples showed a broad endothermic peak around 90 to 95 °C suggesting water loss. The exothermic peak at 250 to 255 °C indicated the complete degradation of GG (Fig. 7b). The additional peak in the commercial sample may be indicative of formulation additives optimized for appropriate gelling. The results are in agreement with the literature reporting complete thermal degradation of the GG around 250 °C (Yang et al. 2013; Viswanathan et al. 2020).

Figure 7c depicts the comparative thermogravimetric analysis of the GG from GGSM81 and commercial sample. The mass loss curve of both samples indicated a similar pattern of thermal degradation. An initial phase of mass reduction up to 25 to 30% in both samples was observed between 30 °C and 245 °C. This phase indicates the dehydration of the GG followed by single sharp loss of mass at temperature range 244 to 265 °C in both the samples with mid-point temperature of 252 °C and 258 °C for commercial and GGSM81 GG. The results are in good agreement with literature (Manda et al. 2018). Both the samples showed only single degradation point followed by plateau curve representing residual inorganic material.

### Microstructure analysis

Figure 8 depicts the surface morphology and qualitative information about the microstructure of the commercial and laboratory produced GG. The particle size of commercial GG was comparatively lower than that from GGSM81. This could be due to oven drying of the laboratory sample which collapses the internal structure of the GG during drying. This could be due to the capillary hydrostatic stress posed by surface tension of the water ebbing from the structure (Dev et al. 2023). The higher magnification explains the pore size, shape, and its distribution. GG from GGSM81 had a more compact than porous structure than commercial

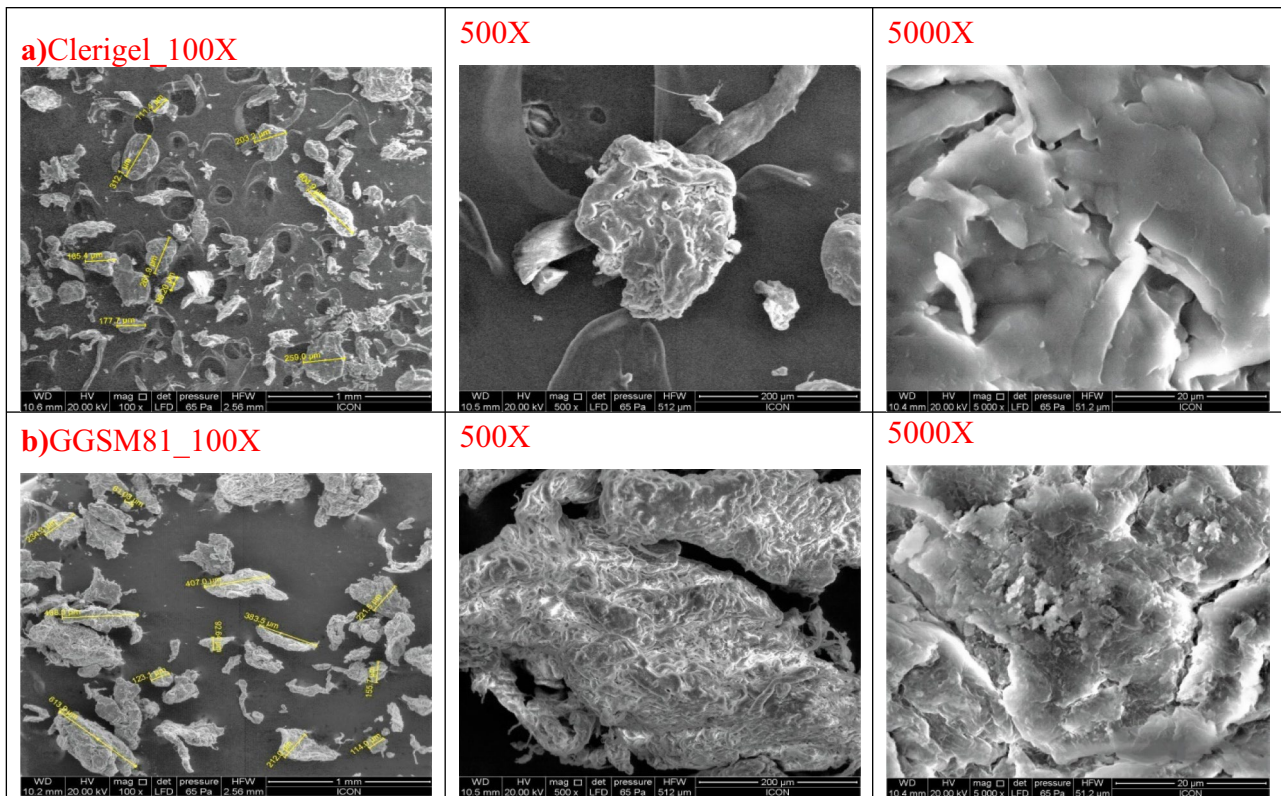


**Fig. 8** Scanning electron microstructure of **a** Clerigel and **b** gellan gum produced by mutant *Shingomonas trueperi* GGSM81

sample. This could also be due to internal structure collapsing at higher drying temperature as well as high rate of drying which resulted in structural packing (Cassanelli et al. 2019).

### Rheological properties

The flow behavior analysis reveals higher consistency index ( $K$ ), yield stress ( $\sigma_0$ ), and apparent viscosity ( $\eta$ ) of the Clerigel than GG from mutant GGSM81 (Table 4, part c). The observations indicate relatively higher viscous nature of the Clerigel than GG from mutant GGSM81 which could be either due to variable molecular weights or chain lengths or due to lack of ionic compounds in GG solution from mutant GGSM81. The effects of molecular weight variation; ionic crosslinker type such as mono, di, or trivalent cations; and their strength on relative viscosity of GG are well reported (Morris et al. 2012; García et al. 2018). However, the shear thinning behavior ( $n$ ) of the GG from mutant GGSM81 was observed to be competitive with Clerigel (Table 4, part c). This confirms its low stickiness and better mouth feel and depicts its applicability in easy to swallow formulations (Dev et al. 2023).

The frequency sweep analysis revealed the storage modulus or elastic modulus ( $G'$ ), loss modulus ( $G''$ ), and loss tangent ( $\tan \delta = G''/G'$ ) over the frequency range of 0.1 to

100 rad/s. The elastic modulus ( $G'$ ) is directly related to bolus formation which is important for the safe and easy swallowing. The GG produced by the mutant strain had comparatively lower elastic modulus ( $G'$ ) than Clerigel (Fig. 9a).

This could be due to presence of ionic components at their optimized concentration in the Clerigel which supports the gel-cluster formation and imparts the strength in material (García et al. 2018). However, GG from mutant shows competitive storage modulus to that of Clerigel with increasing angular frequency. The viscoelastic behavior of these samples can be explained to be due to changes in the macromolecular structure from normal to random helix lead to formation of more complex networking, thereby raising elasticity of material (Morris et al. 2012). Figure 9b depicts the absolute and dominant liquid viscoelastic behavior of the commercial GG over to the solid viscoelastic nature of GG produced by mutant GGSM81 at low frequency range. However, it becomes parallel to each other with increasing frequency. The higher value of the loss tangent ( $> 1$ ) is indicative of the liquid viscoelastic nature whereas its lower value ( $< 1$ ) indicates the solid viscoelastic nature. The increasing angular frequency that reduces the loss factor  $< 1$  is indicative of applicability of the GG produced by mutant GGSM81 as an ingredient in food formulations for dysphagia (Ishihara et al. 2011).

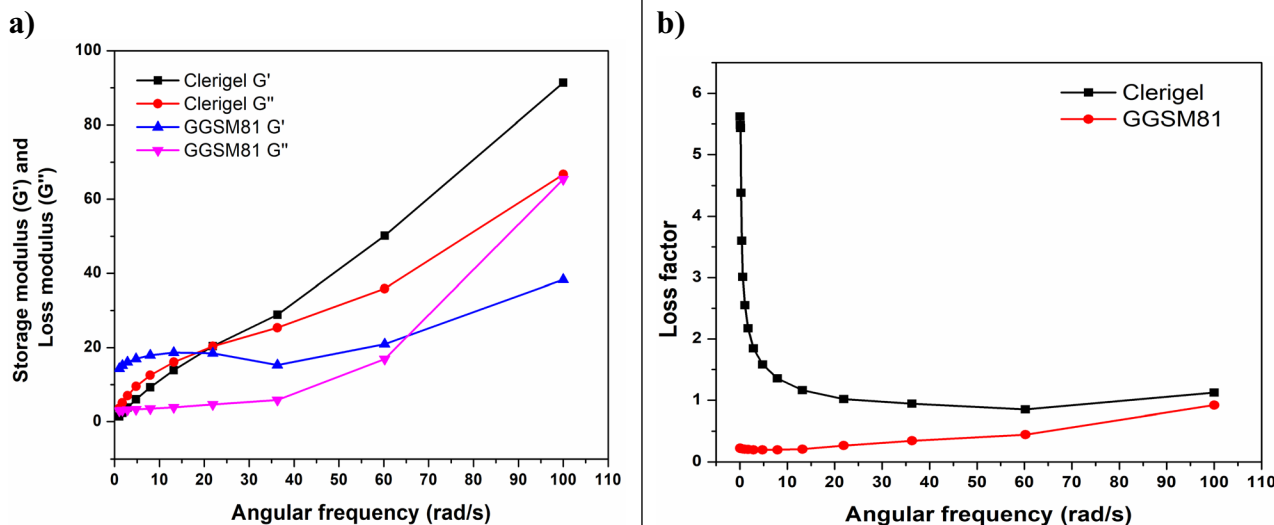


**Fig. 9** Rheological profile of gellan gum from *Sphingomonas trueperi* GGSM81 and Clerigel: **a** storage modulus ( $G'$ ) and loss modulus ( $G''$ ) vs. angular frequency and **b** loss factor vs. angular frequency

## Conclusion

The present study demonstrates the applicability of the random mutational breeding using EMS as mutagen in the development of industrially viable mutants of *Sphingomonas* spp. for the production of gellan gum. The mutant strain was identified as *Sphingomonas trueperi*. Sequential optimization of process parameters and media components yielded almost double (15.6 g/L) gellan gum than wild type strain of *Sphingomonas*. The fermentation profiling at bioreactor level deciphered the role of DOT in gellan fermentation. Bioprocess after upstream optimization yielded  $23 \pm 2.4$  g/L gellan gum with batch productivity of 0.51 g/L/h at 20% DOT. The gellan gum by mutant GGSM81 was characterized for structural and physico-functional attributes and found to be competitive with commercial gellan gum. To the best of our knowledge, this is the first study reporting *Sphingomonas trueperi* as potential producer of gellan gum.

**Supplementary Information** The online version contains supplementary material available at <https://doi.org/10.1007/s10123-023-00399-1>.

**Acknowledgements** Authors would like to acknowledge the research funding under the scheme of Prime Minister's Fellowship for Doctoral Research by HiMedia Laboratories Pvt. Ltd., Mumbai and Science & Engineering Research Board (SERB), Department of Science & Technology (DST), Government of India (GOI) and Confederation of Indian Industry (CII) (SERB/PM Fellow/CII-FICCI/Meeting/2019 dated July 9, 2019). Authors would also like to acknowledge DST-FIST for providing infrastructural facility (Grant reference number: SR/FST/ET-I/2017/67 (C) dated 10-08-2018). Authors are also thankful to Mr. Yogesh Chaudhari for laboratory assistance during bioreactor studies.

**Author contribution** All authors contributed in the study conception and design. Manoj J. Dev: conceptualized, methodology, original draft preparation, software; Girish B. Mahajan: conceptualized, methodology,

supervision and editorial assistance and manuscript finalization; Rahul G. Warke: supervision, data analysis, and investigation; Gangadhar M. Warke: visualization, supervision; Tanuja A. Patil: methodology; Milan R. Satardekar: supervision; Rachana C. Dalvi: methodology; Rekha S. Singhal: conceptualized, supervision, reviewing, and manuscript finalization. All authors have read and approved the manuscript.

**Funding** This research work was funded under the scheme of Prime Minister's Fellowship for Doctoral Research by HiMedia Laboratories Pvt. Ltd., Mumbai and Science & Engineering Research Board (SERB), Department of Science & Technology (DST), Government of India (GOI) and Confederation of Indian Industry (CII) (SERB/PM Fellow/CII-FICCI/Meeting/2019 dated July 9, 2019).

**Data availability** The data will be made available on rational request to corresponding author of the manuscript.

## Declarations

**Competing interests** Manoj J. Dev received fellowship and research infrastructural support from HiMedia Laboratories Pvt. Ltd. India. Rahul G. Warke, Gangadhar M. Warke, Girish B. Mahajan, Tanuja A. Patil, Rachana C. Dalvi, and Milan R. Satardekar report a relationship with HiMedia Laboratories Pvt. Ltd. that includes employment and equity or stocks. Gangadhar M. Warke has patent "Viscous polysaccharide production from microorganisms" (Application number: 202021056610) pending to Indian Patent Office to secure financial outcome from methods, process, and products from the current research work.

## References

Amraoui Y, Prabhu AA, Narisetty V, Coulon F, Kumar Chandel A, Willoughby N, ... Kumar V (2022) Enhanced 2,3-butanediol production by mutant *Enterobacter ludwigii* using Brewers' spent grain hydrolysate: Process optimization for a pragmatic



- biorefinery loom. *Chem Eng J* 427:130851. <https://doi.org/10.1016/j.cej.2021.130851>
- AOAC (2005) Official methods of analysis, 18th edn. Association of Official Analytical Chemists, Rockville, MD, USA
- Arockiasamy S, Banik RM (2008) Optimization of gellan gum production by *Sphingomonas paucimobilis* ATCC 31461 with non-ionic surfactants using central composite design. *J Biosci Bioeng* 105(3):204–210. <https://doi.org/10.1263/jbb.105.204>
- Ashtaputre AA, Shah AK (1995) Studies on the exopolysaccharide from *Sphingomonas paucimobilis*-GS1: nutritional requirements and precursor-forming enzymes. *Curr Microbiol* 31:234–238. <https://doi.org/10.1007/BF00298380>
- Bajaj IB, Saudagar PS, Singhal RS, Pandey A (2006) Statistical approach to optimization of fermentative production of gellan gum from *Sphingomonas paucimobilis* ATCC 31461. *J Biosci Bioeng* 102(3):150–156. <https://doi.org/10.1263/jbb.102.150>
- Bajaj IB, Survase SA, Saudagar PS, Singhal RS (2007) Gellan gum: Fermentative production, downstream processing and applications. *Food Technol Biotechnol* 45(4):341–354
- Banik RM, Santhiagu A (2006) Improvement in production and quality of gellan gum by *Sphingomonas paucimobilis* under high dissolved oxygen tension levels. *Biotech Lett* 28(17):1347–1350. <https://doi.org/10.1007/s10529-006-9098-3>
- Banik RM, Santhiagu A, Upadhyay SN (2007) Optimization of nutrients for gellan gum production by *Sphingomonas paucimobilis* ATCC-31461 in molasses based medium using response surface methodology. *Biores Technol* 98(4):792–797. <https://doi.org/10.1016/j.biortech.2006.03.012>
- Bleisch R, Freitag L, Ihadjadene Y, Sprenger U, Steingröwer J, Walther T, Krujatz F (2022) Strain development in microalgal biotechnology—random mutagenesis techniques. *Life* 12(7):961. <https://doi.org/10.3390/life12070961>
- Cassanelli M, Prosapio V, Norton I, Mills T (2019) Role of the drying technique on the low-acyl gellan gum gel structure: Molecular and macroscopic investigations. *Food Bioprocess Technol* 12:313–324. <https://doi.org/10.1007/s11947-018-2210-6>
- Coelho J, Eusébio D, Gomes D, Frias F, Passarinha LA, Sousa Â (2019) Biosynthesis and isolation of gellan polysaccharide to formulate microspheres for protein capture. *Carbohydr Polym* 220:236–246. <https://doi.org/10.1016/j.carbpol.2019.05.011>
- Coutinho DF, Sant SV, Shin H, Oliveira JT, Gomes ME, Neves NM, ... Reis RL (2010) Modified gellan gum hydrogels with tunable physical and mechanical properties. *Biomater* 31(29):7494–7502. <https://doi.org/10.1016/j.biomaterials.2010.06.035>
- Cupples CG, Cabrera M, Cruz C, Miller JH (1990) A set of *lacZ* mutations in *Escherichia coli* that allow rapid detection of specific frameshift mutations. *Genetics* 125(2):275–280. <https://doi.org/10.1093/genetics/125.2.275>
- Dertli E, Colquhoun IJ, Gunning AP, Bongaerts RJ, Le Gall G, Bonev BB, ... Narbad A (2013) Structure and biosynthesis of two exopolysaccharides produced by *Lactobacillus johnsonii* FI9785. *J Biol Chem* 288(44):31938–31951. <https://doi.org/10.1074/jbc.M113.507418>
- Dev MJ, Warke RG, Warke GM, Mahajan GB, Patil TA, Singhal RS (2022) Advances in fermentative production, purification, characterization and applications of gellan gum. *Bioresour Technol* 359:127498. <https://doi.org/10.1016/j.biortech.2022.127498>
- Dev MJ, Warke RG, Warke GM, Mahajan GB, Singhal RS (2023) Fluidized bed granulation of gellan gum : Investigations of binder effect on physical, structural and rheological properties. *Powder Technol* 415:118199. <https://doi.org/10.1016/j.powtec.2022.118199>
- Devchand M, Gwynne DI (1991) Expression of heterologous proteins in *Aspergillus*. *J Biotechnol* 17(1):3–9. [https://doi.org/10.1016/0168-1656\(91\)90022-N](https://doi.org/10.1016/0168-1656(91)90022-N)
- Faron ML, Buchan BW, Hyke J, Madisen N, Lillie JL, Granato PA, ... Ledebøer NA (2015) Multicenter evaluation of the Bruker MALDI Biotyper CA System for the identification of clinical aerobic Gram-negative bacterial isolates. *PLoS ONE* 10(11):1–13. <https://doi.org/10.1371/journal.pone.0141350>
- Fialho AM, Moreira LM, Granja AT, Popescu AO, Hoffmann K, Sá-Correia I (2008) Occurrence, production, and applications of gellan: current state and perspectives. *Appl Microbiol Biotechnol* 79(6):889–900. <https://doi.org/10.1007/s00253-008-1496-0>
- Foster PL (1991) In vivo mutagenesis. In: Miller (ed), (204):114–125. [https://doi.org/10.1016/0076-6879\(91\)04007-B](https://doi.org/10.1016/0076-6879(91)04007-B)
- García MC, Trujillo LA, Muñoz J, Alfaro MC (2018) Gellan gum fluid gels: Influence of the nature and concentration of gel-promoting ions on rheological properties. *Colloid Polym Sci* 296(11):1741–1748. <https://doi.org/10.1007/s00396-018-4396-6>
- Giavasis L, Harvey LM, McNeil B (2000) Gellan gum. *Crit Rev Biotechnol* 20(3):177–211. <https://doi.org/10.1080/0738850008984169>
- Giavasis I, Harvey LM, McNeil B (2006) The effect of agitation and aeration on the synthesis and molecular weight of gellan in batch cultures of *Sphingomonas paucimobilis*. *Enzyme Microb Technol* 38(1–2):101–108. <https://doi.org/10.1016/j.enzmictec.2005.05.003>
- Hamcerencu M, Desbrieres J, Khoukh A, Popa M, Riess G (2008) Synthesis and characterization of new unsaturated esters of gellan gum. *Carbohydr Polym* 71(1):92–100. <https://doi.org/10.1016/j.carbpol.2007.05.021>
- Hestrin S (1949) The reaction of acetylcholine and other carboxylic acid derivatives with hydroxylamine, and its analytical application. *J Biol Chem* 180(1):249–261. [https://doi.org/10.1016/s0021-9258\(18\)56740-5](https://doi.org/10.1016/s0021-9258(18)56740-5)
- Huang J, Zhu S, Li C, Zhang C, Ji Y (2020) Cost-effective optimization of gellan gum production by *Sphingomonas paucimobilis* using corn steep liquor. *Prep Biochem Biotechnol* 50(2):191–197. <https://doi.org/10.1080/10826068.2019.1692215>
- Huang J, Jiang S, Xu X, Wu H, Zhu X, Ke Z, ... Xu Z (2012) Effects of carbon/nitrogen ratio, dissolved oxygen and impeller type on gellan gum production in *Sphingomonas paucimobilis*. *Ann Microbiol* 62(1):299–305. <https://doi.org/10.1007/s13213-011-0261-2>
- Ishihara S, Nakauma M, Funami T, Odake S, Nishinari K (2011) Swallowing profiles of food polysaccharide gels in relation to bolus rheology. *Food Hydrocoll* 25:1016–1024. <https://doi.org/10.1016/j.foodhyd.2010.09.022>
- Jay AJ, Colquhoun IJ, Ridout MJ, Brownsey GJ, Morris VJ, Fialho AM, ... Sá-Correia I (1998) Analysis of structure and function of gellans with different substitution patterns. *Carbohydr Polym* 35(3–4):179–188. [https://doi.org/10.1016/S0144-8617\(97\)00241-5](https://doi.org/10.1016/S0144-8617(97)00241-5)
- Kamer DDA, Gumus T, Palabiyyik I, Demirci AS, Oksuz O (2021) Grape pomace as a promising source for gellan gum production. *Food Hydrocoll* 114:106584. <https://doi.org/10.1016/j.foodhyd.2020.106584>
- Kanari B, Banik RR, Upadhyay SN (2002) Effect of environmental factors and carbohydrate on gellan gum production. *Appl Biochem Biotechnol* 102(1):129–140. <https://doi.org/10.1385/ABAB:102-103:1-6:129>
- Kothari V, Mishra T, Kushwah P (2014) Mutagenic effect of microwave radiation on exopolysaccharide production in *Xanthomonas campestris*. *Curr Trends Biotechnol Pharm* 8(1):29–37
- Kuo MS, Mort AJ, Dell A (1986) Identification and location of L-glycerate, an unusual acyl substituent in gellan gum. *Carbohydr Res* 156:173–187. [https://doi.org/10.1016/S0008-6215\(00\)90109-5](https://doi.org/10.1016/S0008-6215(00)90109-5)
- Li X, Zhao S, Chen L, Zhou Q, Qiu J, Xin X, Zhang Y, Yuan W, Tian C, Yang J, Yu X (2023) High-level production of pullulan from high concentration of glucose by mutagenesis and adaptive laboratory evolution of *Aureobasidium pullulans*. *Carbohydr Polym* 302:120426. <https://doi.org/10.1016/j.carbpol.2022.120426>
- Li A, Hu T, Luo H, Alam N, Xin J, Li H, ... Li O (2019) A carotenoid- and poly-hydroxybutyrate-free mutant strain of *Sphingomonas*

- elodea* ATCC 31461 for the commercial production of gellan. *mSphere* 4(5):1–11. <https://doi.org/10.1128/mSphere.00668-19>
- Lin R, Liu H, Wu S, Pang L, Jia M, Fan K, ... Jia L (2012) Production and in vitro antioxidant activity of exopolysaccharide by a mutant, *Cordyceps militaris* SU5–08. *Int J Biol Macromol* 51(1–2):153–157. <https://doi.org/10.1016/j.jbiomac.2012.04.011>
- Lobas D, Schumpe S, Deckwer WD (1992) The production of gellan exopolysaccharide with *Sphingomonas paucimobilis* E2 (DSM 6314). *Appl Microbiol Biotechnol* 37(4):411–415. <https://doi.org/10.1007/BF00180959>
- Manda MG, da Silva LP, Cerqueira MT, Pereira DR, Oliveira MB, Mano JF, ... Reis RL (2018) Gellan gum-hydroxyapatite composite spongy-like hydrogels for bone tissue engineering. *J Biomed Mater Res A* 106(2):479–490. <https://doi.org/10.1002/jbm.a.36248>
- Martins LO, Sá-Correia I (1994) Temperature profiles of gellan gum synthesis and activities of biosynthetic enzymes I. *Biotechnol Appl Biochem* 20(3):385–395. <https://doi.org/10.1111/j.1470-8744.1994.tb00324.x>
- Matsuyama H, Kamesaki T, Sasaki R, Minami H, Yumoto I (2003) Production of two types of exopolysaccharide by *Novosphingobium rosa*. *J Biosci Bioeng* 95(2):152–156. <https://doi.org/10.1263/jbb.95.152>
- Miranda AL, Costa SS, Assis DDJ, de Jesus CS, Guimarães AG, Druzian JI (2020) Influence of strain and fermentation time on the production, composition, and properties of xanthan gum. *J Appl Polym Sci* 137(15):48557. <https://doi.org/10.1002/app.48557>
- Mitra R, Dutta D (2018) Growth profiling, kinetics and substrate utilization of low-cost dairy waste for production of  $\beta$ -cryptoxanthin by *Kocuria marina* DAGII. *Royal Soc Open Sci* 5(7):172318. <https://doi.org/10.1098/rsos.172318>
- Monteiro GA, Fialho AM, Ripley SJ, Sá-Correia I (1992) Electrotransformation of gellan-gum producing and non-producing *Pseudomonas elodea* strains. *J Appl Bacteriol* 72(5):423–428. <https://doi.org/10.1111/j.1365-2672.1992.tb01855.x>
- Morris ER, Nishinari K, Rinaudo M (2012) Gelation of gellan - A review. *Food Hydrocoll* 28(2):373–411. <https://doi.org/10.1016/j.foodhyd.2012.01.004>
- Nampoothiri KM, Singhanian RR, Sabarinath C, Pandey A (2003) Fermentative production of gellan using *Sphingomonas paucimobilis*. *Process Biochem* 38(11):1513–1519. [https://doi.org/10.1016/S0032-9592\(02\)00321-7](https://doi.org/10.1016/S0032-9592(02)00321-7)
- Naveena B, Gopinath KP, Sakthiselvan P, Partha N (2012) Enhanced production of thrombinase by *Streptomyces venezuelae*: Kinetic studies on growth and enzyme production of mutant strain. *Biores Technol* 111:417–424. <https://doi.org/10.1016/j.biortech.2012.02.056>
- O'Neill MA, Selvendran RR, Morris VJ (1983) Structure of the acidic extracellular gelling polysaccharide produced by *Pseudomonas elodea*. *Carbohydr Res* 124(1):123–133. [https://doi.org/10.1016/0008-6215\(83\)88360-8.43](https://doi.org/10.1016/0008-6215(83)88360-8.43)
- Osmalek T, Froelich A, Tasarek S (2014) Application of gellan gum in pharmacy and medicine. *Int J Pharm* 466(1–2):328–340. <https://doi.org/10.1016/j.ijpharm.2014.03.038>
- Prajapati VD, Jani GK, Zala BS, Khutliwala TA (2013) An insight into the emerging exopolysaccharide gellan gum as a novel polymer. *Carbohydr Polym* 93(2):670–678. <https://doi.org/10.1016/j.carbpol.2013.01.030>
- Raghunandan K, Kumar A, Kumar S, Permaul K, Singh S (2018) Production of gellan gum, an exopolysaccharide, from biodiesel-derived waste glycerol by *Sphingomonas* spp. *3 Biotech* 8(1):1–13. <https://doi.org/10.1007/s13205-018-1096-3>
- Reid SJ, Abratt VR (2005) Sucrose utilisation in bacteria: Genetic organisation and regulation. *Appl Microbiol Biotechnol* 67:312–321. <https://doi.org/10.1007/s00253-004-1885-y>
- Sega GA (1984) A review of the genetic effects of ethyl methanesulfonate. *Mutat Res/Rev Gen Toxicol* 134(2–3):113–142. [https://doi.org/10.1016/0165-1110\(84\)90007-1](https://doi.org/10.1016/0165-1110(84)90007-1)
- Sengupta D, Datta S, Biswas D (2018) Towards a better production of bacterial exopolysaccharides by controlling genetic as well as physico-chemical parameters. *Appl Microbiol Biotechnol* 102:1587–1598. <https://doi.org/10.1007/s00253-018-8745-7>
- Sudhamani SR, Prasad MS, UdayaSankar K (2003) DSC and FTIR studies on gellan and polyvinyl alcohol (PVA) blend films. *Food Hydrocoll* 17(3):245–250. [https://doi.org/10.1016/S0268-005X\(02\)00057-7](https://doi.org/10.1016/S0268-005X(02)00057-7)
- Sukumar S, Arockiasamy S, Moothona MC (2021) Optimization of cultural conditions of gellan gum production from recombinant *Sphingomonas paucimobilis* ATCC 31461 and its characterization. *J Appl Biol Biotechnol* 9(1):58–67. <https://doi.org/10.7324/JABB.2021.9108>
- Viswanathan HS, Syed Abdul Rahman S, Venkatachalam P, Karupiah S (2020) Production of gellan gum using milk skin residue (MSR)—a tea shop waste: Statistical optimization and downstream processing. *Biomass Convers Biorefin* 1–15. <https://doi.org/10.1007/s13399-020-01026-z>
- Wang X, Xu P, Yuan Y, Liu C, Zhang D, Yang Z, ... Ma C (2006) Modeling for gellan gum production by *Sphingomonas paucimobilis* ATCC 31461 in a simplified medium. *Appl Environ Microbiol* 72(5):3367–3374. <https://doi.org/10.1128/AEM.72.5.3367-3374.2006>
- Wang D, Kim H, Lee S, Kim DH, Joe MH et al (2020) Improved gellan gum production by a newly-isolated *Sphingomonas azotifigens* GL-1 in a cheese whey and molasses based medium. *Process Biochemistry* 95:269–278. <https://doi.org/10.1016/j.procbio.2020.02.020>
- West TP, Fullenkamp NA (2001) Effect of culture medium pH on bacterial gellan production. *Microbios* 105(412):133–140
- Wilson K (2001) Preparation of genomic DNA from bacteria. *Curr Protoc Mol Biol* 56(1):2–4. <https://doi.org/10.1002/0471142727.mb0204s56>
- Wu X, Li O, Chen Y, Zhu L, Qian C, Teng Y, Tao X (2011) A carotenoid-free mutant strain of *Sphingomonas paucimobilis* ATCC 31461 for the commercial production of gellan. *Carbohydr Polym* 84(3):1201–1207. <https://doi.org/10.1016/j.carbpol.2011.01.018>
- Yang F, Xia S, Tan C, Zhang X (2013) Preparation and evaluation of chitosan-calcium-gellan gum beads for controlled release of protein. *Eur Food Res Technol* 237(4):467–479. <https://doi.org/10.1007/s00217-013-2021-y>
- Zhang HT, Zhu L, Liu D, Zhan XB, Ding J, Lin CC (2015) Model-based estimation of optimal dissolved oxygen profile in *Agrobacterium* sp. fed-batch fermentation for improvement of curdlan production under nitrogen-limited condition. *Biochem Eng J* 103:12–21. <https://doi.org/10.1016/j.bej.2015.06.012>
- Zhu L, Wu X, Li O, Chen Y, Qian C, Teng Y, ... Gao H (2011) Cloning and knockout of phytoene desaturase gene in *Sphingomonas elodea* ATCC 31461 for economic recovery of gellan gum. *J Ind Microbiol Biotechnol* 38(9):1507–1513. <https://doi.org/10.1007/s10295-010-0937-9>

**Publisher's note** Springer Nature remains neutral with regard to jurisdictional claims in published maps and institutional affiliations.

Springer Nature or its licensor (e.g. a society or other partner) holds exclusive rights to this article under a publishing agreement with the author(s) or other rightsholder(s); author self-archiving of the accepted manuscript version of this article is solely governed by the terms of such publishing agreement and applicable law.